Geochemistry, Geophysics, Geosystems

RESEARCH ARTICLE

10.1002/2015GC006199

Distinct responses of planktonic foraminiferal B/Ca to dissolution on seafloor

Yuhao Dai[1], Jimin Yu[1], and Heather J. H. Johnstone[2]

[1]Research School of Earth Sciences, Australian National University, Canberra, Australian Capital Territory, Australia, [2]MARUM—Center for Marine Environmental Sciences, University of Bremen, Bremen, Germany

Key Points:
- We present new core-top B/Ca in four planktonic foraminiferal species from three depth transects
- B/Ca ratios in different planktonic species respond distinctly to dissolution
- Methods are proposed to correct for dissolution effects on planktonic B/Ca

Supporting Information:
- Supporting Information S1

Correspondence to:
Y. Dai,
yuhao.dai@anu.edu.au

Citation:
Dai, Y., J. Yu, and H. J. H. Johnstone (2016), Distinct responses of planktonic foraminiferal B/Ca to dissolution on seafloor, *Geochem. Geophys. Geosyst.*, *17*, 1339–1348, doi:10.1002/2015GC006199.

Received 23 NOV 2015
Accepted 10 MAR 2016
Accepted article online 14 MAR 2016
Published online 17 APR 2016

Abstract We have measured B/Ca in four core-top planktonic foraminiferal species (*Globigerinoides ruber* (white), *Globigerinoides sacculifer* (without final sac-like chamber), *Neogloboquadrina dutertrei*, and *Pulleniatina obliquiloculata*) from three depth transects (the Caribbean Sea, the southwestern Indian Ocean, and the Ontong Java Plateau) to evaluate the effect of dissolution on planktonic foraminiferal B/Ca. At each transect, *G. ruber* (w) and *G. sacculifer* (w/o sac) show decreasing B/Ca with increasing water depth. This decrease in B/Ca is accompanied with decreases in shell weights, Mg/Ca, and bottom water calcite saturation state. This indicates a postdepositional dissolution effect on B/Ca in these two species. The strong correlation observed between changes in B/Ca and bottom water calcite saturation state offers an approach to correcting for the dissolution bias. By contrast, B/Ca in *N. dutertrei* and *P. obliquiloculata* remains unchanged along depth transects, although shell weights and Mg/Ca display significant declines. Overall, our core-top results suggest species-specific dissolution effects on B/Ca in different planktonic foraminiferal species.

1. Introduction

It is well documented that trace element to calcium ratios of foraminiferal shells can be altered by partial dissolution on seafloor [*Russell et al*., 1994; *Brown and Elderfield*, 1996; *Dekens et al*., 2002; *Regenberg et al*., 2006]. Therefore, dissolution can alter the geochemical signature of foraminiferal calcite and possibly bias paleoceanographic reconstructions. Several studies have revealed significant dissolution effects on planktonic foraminiferal B/Ca, a recently developed proxy for surface seawater carbonate chemistry [*Yu et al*., 2007a; *Allen et al*., 2011, 2012]. B/Ca in both extant and extinct planktonic foraminiferal species is reported to be affected by postdepositional processes on seafloor [*Wara et al*., 2003; *Seki et al*., 2010; *Coadic et al*., 2013; *Edgar et al*., 2015]. Other existing data, although limited, appear to suggest little influence of dissolution on B/Ca in some planktonic species. For example, a few core-top data from the North Atlantic show that B/Ca in *Globorotalia inflata* is resistant to dissolution [*Yu et al*., 2007a].

For reliable reconstructions, it is necessary to evaluate the influence of postmortem dissolution on B/Ca in different species. At present, available data are insufficient to fully explore the dissolution effect on B/Ca in different planktonic foraminiferal species. To fill in this gap, we measure B/Ca in four planktonic foraminiferal species commonly used in paleoceanographic reconstructions from core-top samples along three depth transects from the three major ocean basins. The aim of this study is to test whether there are species-specific dissolution effects on B/Ca in different planktonic foraminiferal species.

2. Materials and Methods

2.1. Samples

In this study, we present B/Ca in four planktonic species: *Globigerinoides sacculifer* (w/o sac), *Globigerinoides ruber* (white), *Neogloboquadrina dutertrei*, and *Pulleniatina obliquiloculata*. Mg/Ca and shell weights for the samples used in this study were previously published [*Johnstone et al*., 2010, 2011]. These species are chosen based on their living habitats, symbiont conditions, shell wall structure, and resistance to dissolution. *G. sacculifer* (w/o sac) and *G. ruber* (w) are spinose species that inhabit in the surface mixed layer, harboring dinoflagellates as symbiont [*Hemleben et al*., 1989], and their shells are susceptible to dissolution according to the planktonic foraminifer solubility ranking of *Berger* [1970], which is based on observations from dissolution field experiments and species assemblage shifts in sediment under variable saturation conditions.

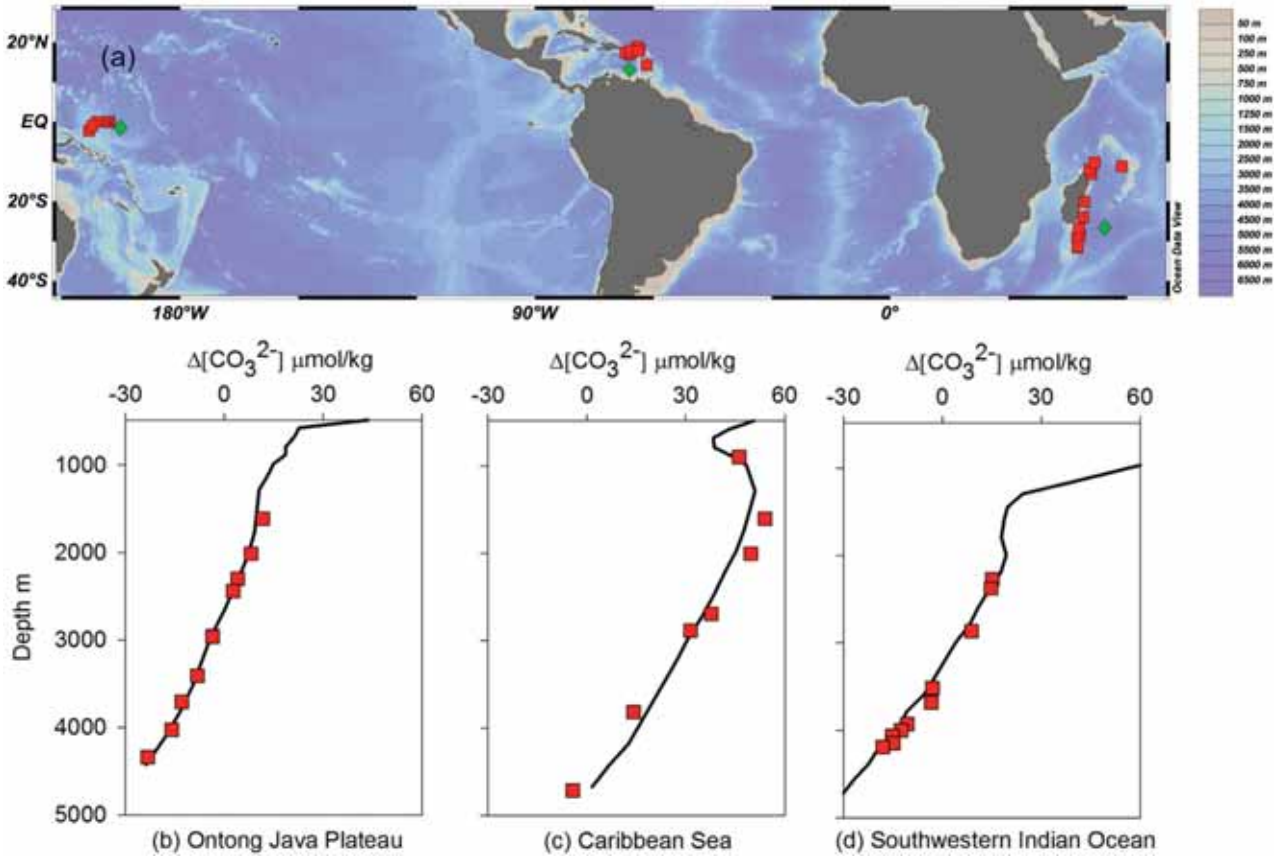

Figure 1. Hydrology of the core-tops used in this study. (a) Location of the core-tops (red squares) and nearby GLODAP stations (green diamonds) selected for $\Delta[CO_3^{2-}]$ profiles; (b–d) $\Delta[CO_3^{2-}]$ of core-tops plotted with $\Delta[CO_3^{2-}]$ depth profile of a nearby GLODAP station for three depth transects.

N. dutertrei and *P. obliquiloculata* are nonspinose species living in the thermocline, harboring chrysophycophytes as symbiont, and their shells are more resistant to dissolution compared to those of *G. ruber* and *G. sacculifer* [*Berger*, 1970; *Gastrich*, 1987; *Hemleben et al*., 1989].

Foraminiferal shells analyzed in this study are from 28 core-top samples obtained from three depth transects in the Caribbean Sea, the southwestern Indian Ocean, and the Ontong Java Plateau (Figure 1). All core-tops are verified to be Holocene in age, and the age difference within the Caribbean Sea and the southwestern Indian Ocean transect sites is smaller than 3 kyr [*Regenberg et al*., 2006; *Wilson et al*., 2012] (see supporting information Table S1 for details). Due to the constrained geographic coverage of core-top samples, we assume minimal environmental variability in surface conditions during calcification and therefore trace element compositions (B/Ca and Mg/Ca) of shells between sites along each transect. Nevertheless, it should be noted that compared to the Caribbean Sea and the Ontong Java Plateau transects, samples from the southwestern Indian Ocean cover a wider geographic region, which could cause some variations in the "initial" B/Ca in foraminiferal shells. Excluding data from the Indian Ocean depth transect would not affect our conclusions.

2.2. B/Ca Measurements

For each trace element to calcium ratio analysis, approximately 30 tests were picked from a narrow size fraction of 300–355 μm to minimize size potential size-related effects on B/Ca and Mg/Ca [*Elderfield et al*., 2002; *Ni et al*., 2007]. Foraminiferal shells were cleaned following the "Mg-cleaning" procedure which includes clay/silicate removal, oxidative cleaning, and weak acid leaching steps [*Barker et al*., 2003]. B/Ca was measured on an ICP-MS following procedure by *Yu et al*. [2005] and *Yu et al*. [2007b]. Based on replicate analyses of a consistency standard, the precision of B/Ca is 3% at 95% confidence interval (151.4 ± 4.2 μmol/mol,

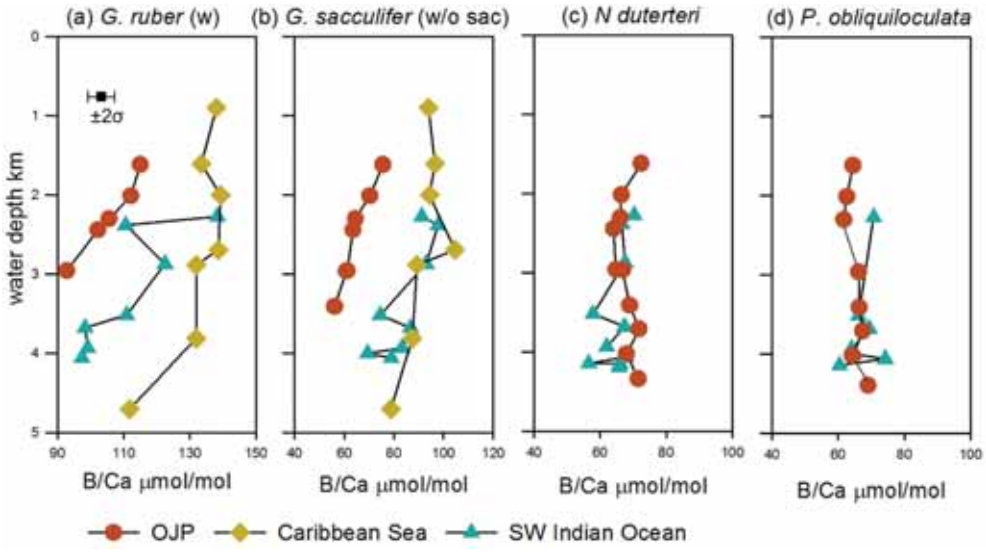

Figure 2. Planktonic B/Ca in four species against water depth from three depth transects: (a) *G. ruber* (w), (b) *G. sacculifer* (w/o sac), (c) *N. dutertrei*, and (d) *P. obliquiloculata*. Error bar in Figure 2a represents $\pm 2\sigma$ range of the consistent standard.

2 s.d.). Mn/Ca, Fe/Ca, and Al/Ca were also measured to monitor possible contamination from Mn or Fe oxyhydroxide-coatings and the effectiveness of clay removal. We found no correlation between B/Ca and these element/Ca ratios, suggesting minimal influences from contaminating phases.

2.3. Hydrological Data Calculations

Bottom water calcite saturation states, $\Delta[CO_3^{2-}]$, defined as $\Delta[CO_3^{2-}] = [CO_3^{2-}]_{\text{in situ}} - [CO_3^{2-}]_{\text{saturated}}$, were estimated using data from the Global Ocean Data Analysis Project (GLODAP) database [*Key et al.*, 2004]. Anthropogenic CO_2 was removed to derive preindustrial dissolved inorganic carbon (DIC) [*Sabine et al.*, 2004]. Bottom water $\Delta[CO_3^{2-}]$ were calculated using CO2sys.xls [*Pelletier et al.*, 2005], following the method and constants used previously [*Yu and Elderfield*, 2007]. Our calculation reveals a large range in bottom water $\Delta[CO_3^{2-}]$ from -23 to 54 μmol/kg at the three depth transects, making these core-top samples ideal to investigate dissolution effects on B/Ca.

3. Results

In the Caribbean Sea, B/Ca in *G. ruber* (w) remains roughly stable at 135 ± 4 μmol/mol above 3.8 km (1 standard deviation, the same below), and is lowered by ~23 μmol/mol (~17%) from 3.8 to 5.0 km (Figure 2 and Table 1). For the southwestern Indian and the Ontong Java Plateau transects, B/Ca in *G. ruber* (w) appears to show a continuous decline throughout the entire depth ranges. B/Ca in *G. ruber* (w) decreases by ~20% from 1.6 to 3.0 km depth at the Ontong Java Plateau, and by ~30% from 2.3 to 4.1 km depth in the southwestern Indian Ocean. Large scatter in B/Ca is seen between 2 and 3 km water depth at the Indian Ocean transect, perhaps reflecting less homogeneous surface conditions associated with these core-tops.

Similar trends are observed in *G. sacculifer* (w/o) from these three depth transects. At the Caribbean Sea depth transect, *G. sacculifer* (w/o sac) shows stable B/Ca of 94 ± 6 μmol/mol above 3.8 km and a ~15 μmol/mol (~16%) decline below this depth. B/Ca in *G. sacculifer* (w/o sac) decreases by ~26% from 1.6 to 3.7 km at the Ontong Java Plateau, and by ~24% from 2.3 to 4.1 km in the southwestern Indian Ocean.

In contrast, *N. dutertrei* and *P. obliquiloculata* show no decreasing trend in B/Ca with water depth at the two depth transects in the Indian and Pacific Oceans. Instead, B/Ca in these two species exhibit stable values. At the Ontong Java Plateau, B/Ca is 68 ± 3 μmol/mol and 65 ± 2 μmol/mol in *N. dutertrei* and *P. obliquiloculata*,

Table 1. B/Ca in Four Species From Three Depth Transects

	Planktonic Foraminiferal B/Ca μmol/mol			
Core	*G. ruber* (w)	*G. sacculifer* (w/o sac)	*N. dutertrei*	*P. obliquiloculata*
Ontong Java Plateau				
1BC3	115	75	72	64
1.5BC33	112	70	66	63
2BC13	106	64	66	62
2.5BC37	102	63	64	
3BC16	93	61	65	
3BC24	106	61	67	66
4BC51		56	69	66
4.5BC53			72	67
5BC54			68	64
5.5BC58			71	
6BC66				69
Southwestern Indian Ocean				
WIND 20B	138	91	70	71
WIND 11B	111	98	67	
WIND 10B	122	93	67	
WIND 33B	111	74	58	66
WIND 5B	98	87	67	69
WIND 25B	99	83	62	64
WIND 23B		69		65
WIND 13B	97	79	68	74
WIND 28B			56	60
WIND 6B			66	
WIND 12B			66	
Caribbean Sea				
M35013-3	138	94		
M35014-1	133	96		
M35020-1	139	94		
M35010-2	139	104		
M35004-1	132	89		
M35026-2	132	87		
M35024-6	112	79		

respectively. In the southwestern Indian Ocean, B/Ca is 65 ± 4 μmol/mol and 67 ± 5 μmol/mol in *N. dutertrei* and *P. obliquiloculata*, respectively.

4. Discussion

4.1. Species-Specific Dissolution Effect on Planktonic B/Ca

Previous studies have shown that post-depositional dissolution in corrosive bottom waters can significantly lower shell weights and Mg/Ca of the species used in this study [*Broecker and Clark*, 2001a; *de Villiers*, 2005; *Regenberg et al*., 2006; *Johnstone et al*., 2010, 2011]. Therefore, we employ shell weights and Mg/Ca as indicators of dissolution in this study. B/Ca in *G. sacculifer* (w/o sac) and *G. ruber* (w) strongly correlates with Mg/Ca and shell weight at the Ontong Java Plateau (see Figure 3 and Table 2, $r^2 = 0.94$ with shell weight, $r^2 = 0.60$ with Mg/Ca for *G. sacculifer* (w/o sac); $r^2 = 0.84$ with shell weight, $r^2 = 0.62$ with Mg/Ca for *G. ruber* (w)). In the southwestern Indian Ocean, B/Ca in these two species sometimes show relatively poor correlations with Mg/Ca and shell weight, possibly due to large variations in their initial values. Despite the scatter, the overall decreasing trend of B/Ca with decreasing shell weight and Mg/Ca is similar to that seen at Ontong Java Plateau. Because the decreases in shell weight and Mg/Ca are thought to be resulted from dissolution on seafloor, we suggest that the decrease in B/Ca with increasing water depth observed in *G. sacculifer* (w/o sac) and *G. ruber* (w) is a response to the same process. This is consistent with the previous observation on *G. sacculifer* [*Seki et al*., 2010; *Coadic et al*., 2013].

In contrast, B/Ca in *N. dutertrei* and *P. obliquiloculata* remains invariant, while shell weights and Mg/Ca exhibit significant changes. In the southwestern Indian Ocean and the Ontong Java Plateau, shell weights of *N. dutertrei* and *P. obliquiloculata* decline 38–50% and 31–40% from the lowest to deepest sites, respectively; Mg/Ca in *dutertrei* and *P. obliquiloculata* declines 41–61% and 53–57%, respectively. Minimal change in B/Ca associated with substantial declines in shell weights and Mg/Ca suggests that B/Ca in these two species is not sensitive to dissolution. Similarly, dissolution appears to impose little influence on B/Ca in *G. inflata* [*Yu et al*., 2007a].

Our results suggest that dissolution effects on planktonic foraminiferal B/Ca are species specific. B/Ca in spinose mixed layer dwellers, *G. ruber* (w) and *G. sacculifer* (w/o sac), is sensitive to dissolution. On the contrary, B/Ca in nonspinose thermocline dwellers, *G. inflata*, *N. dutertrei*, and *P. obliquiloculata*, is not sensitive to dissolution.

4.2. Reasons for Different Dissolution Responses

Dissolution of foraminiferal shell is a selective process, in which more soluble parts of the shell are preferentially removed. As high-Mg phase is known to be more soluble than low-Mg phase in foraminiferal calcite [*Brown and Elderfield*, 1996; *Bassinot et al*., 2004; *Nouet and Bassinot*, 2007; *Johnstone et al*., 2011] and Mg is heterogeneously distributed within shells of planktonic species [*Eggins et al*., 2003; *Sadekov et al*., 2005; *Branson et al*., 2013], dissolution on the seafloor can lower Mg/Ca in various planktonic species [*Regenberg*

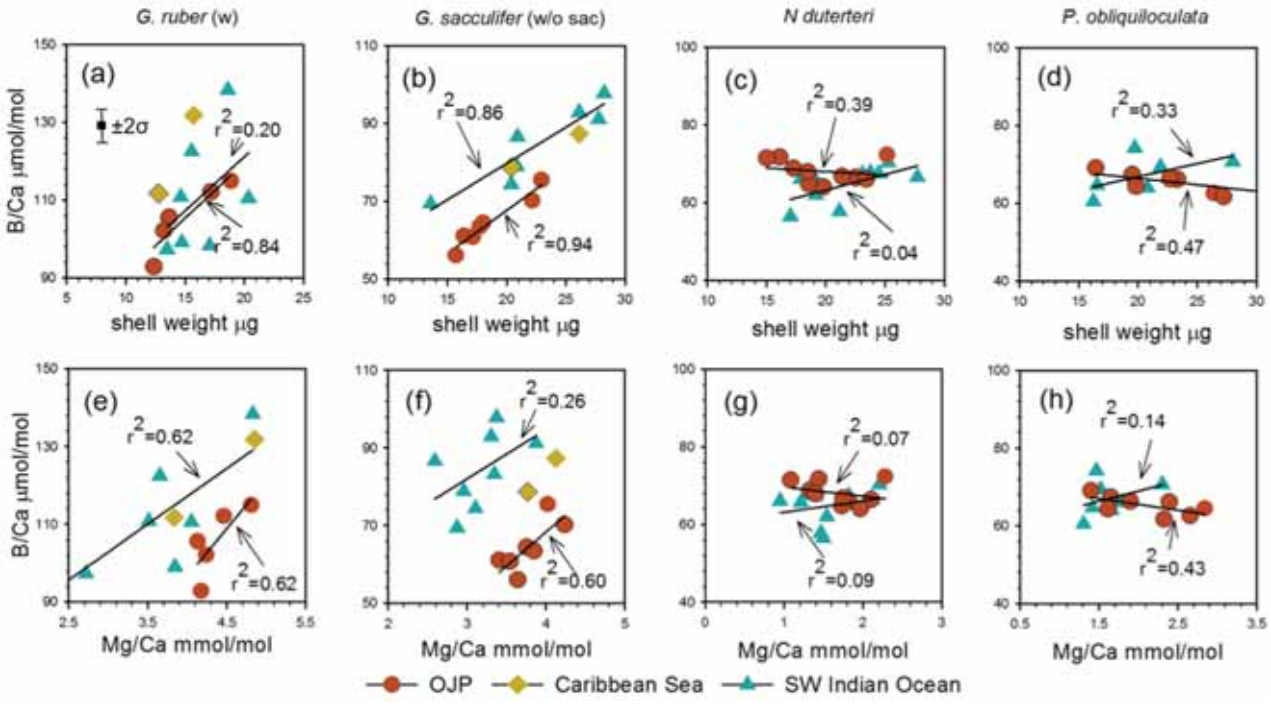

Figure 3. Planktonic B/Ca versus (a–d) shell weight and (e–h) Mg/Ca. In the Caribbean Sea, only data with $\Delta[CO_3^{2-}]$ lower than critical $\Delta[CO_3^{2-}]$ for dissolution are shown (see section 4.3). Solid lines show the best linear fit of data. Error bar in Figure 4a represents $\pm 2\sigma$ range of the consistent standard. B/Ca in *G. ruber* (w) and *G. sacculifer* (w/o sac) are significantly correlated with shell weight and Mg/Ca, suggesting strong dissolution effects on B/Ca in these two species. By contrast, no significant correlation is observed for B/Ca in *N. dutertrei* or *P. obliquiloculata*, implying negligible dissolution influence on B/Ca in these species. Shell weight data are from *Johnstone et al.* [2010]; Mg/Ca data are from *Johnstone et al.* [2011].

et al., 2014]. A similar dissolution effect on B/Ca in *G. ruber* (w) and *G. sacculifer* (w/o sac) to that observed for Mg/Ca would suggest that B is not homogeneously distributed within shells of these species and that high-B phases are preferentially removed by dissolution. The distribution of B within the foraminiferal shell has been investigated in two species: symbiont-bearing planktonic species *Orbulina universa* and symbiont-bearing benthic species *Amphistegina lessonii* [*Allen et al.*, 2011; *Branson et al.*, 2015]. B banding was observed in both species. It is reasonable to speculate that B banding is also present within shell of *G. ruber* (w) and *G. sacculifer* (w/o sac). Existing studies do not allow faithful speculation of the B distribution within shells of nonspinose species examined in this study. Nevertheless, if B is preferentially removed by dissolution, the minimal dissolution effect on B/Ca in nonspinose species would suggest that B is relatively homogeneously distributed within shells of these species.

The reasons for different distribution patterns of boron within foraminiferal shells might be related to symbiont activities. According to studies on $\delta^{11}B$, pH of the microenvironment surrounding the foraminifera shell can be elevated by symbiont activities [*Hönisch et al.*, 2003; *Zeebe et al.*, 2003; *Rollion-Bard and Erez*, 2010]. When pH within the calcifying fluid is raised by the high rate of photosynthesis activity, more B would be incorporated into the foraminiferal shell, because the concentration of $B(OH)_4^-$, the presumed boron species that is incorporated in the foraminiferal shell, is raised [*Hemming and Hanson*, 1992]. *G. ruber* and *G. sacculifer* have strong symbiont activities, so that diurnal changing symbiont activities could generate heterogeneity of B within shells. Although *N. dutertrei* and *P. obliquiloculata* also harbor algal [*Gastrich*, 1987], the associated symbiont activity is weaker because they calcify at deeper depths where light intensity is much reduced. Therefore, it is reasonable that B is more homogeneously distributed within shell of these two deeper dwelling species.

4.3. Correlation With Bottom Water $\Delta[CO_3^{2-}]$

Under-saturated conditions with respect to carbonate ion can result in the dissolution of planktonic foraminiferal shells on seafloor [*Berger*, 1970; *Brown and Elderfield*, 1996]. Decreases in shell weight and Mg/Ca are initiated above the calcite saturation horizon at a threshold $\Delta[CO_3^{2-}]$ value [*Lohmann*, 1995; *Broecker et al.*,

Table 2. Summary of Regression Analyses

Location	Slope	r^2	n	t ($\alpha = 0.05$)	P
1. B/Ca-Shell Weight					
G. sacculifer (w/o sac)					
SW Indian	1.9 ± 0.3	0.86	8	6.07	<0.001
OJP	2.2 ± 0.3	0.94	7	8.85	<0.001
G. ruber (w)					
SW Indian	2.8 ± 2.4	0.20	7	1.12	0.264
OJP	2.8 ± 0.7	0.84	6	4.58	<0.001
N. dutertrei					
SW Indian	−0.2 ± 0.3	0.04	10	0.58	0.564
OJP	0.8 ± 0.4	0.39	10	2.26	0.024
P. obliquiloculata					
SW Indian	0.7 ± 0.4	0.33	7	1.57	0.117
OJP	−0.3 ± 0.1	0.47	8	2.31	0.021
2. B/Ca-Mg/Ca					
G. sacculifer (w/o sac)					
SW Indian	12.7 ± 8.8	0.26	8	1.45	0.093
OJP	17.5 ± 6.5	0.60	7	2.69	0.016
SLR[a]	15.8 ± 2.3	0.91	7	6.94	<0.001
G. ruber (w)					
SW Indian	14.3 ± 5.0	0.62	7	2.84	0.012
OJP	24.0 ± 9.7	0.62	6	2.46	0.024
N. dutertrei					
SW Indian	3.0 ± 3.9	0.07	10	0.76	0.233
OJP	−2.3 ± 2.7	0.09	10	0.88	0.200
P. obliquiloculata					
SW Indian	5.2 ± 5.8	0.14	7	0.91	0.198
OJP	−3.0 ± 1.4	0.43	8	2.14	0.033
3. B/Ca-ΔCO_3^{2-}					
G. sacculifer (w/o sac)					
SW Indian	0.68 ± 0.17	0.74	8	4.09	0.002
OJP	0.90 ± 0.09	0.95	7	9.72	<0.001
SLR[a]	0.32 ± 0.06	0.90	5	5.20	0.002
G. ruber (w)					
SW Indian	0.64 ± 0.28	0.57	6	2.32	0.030
OJP	1.01 ± 0.35	0.68	6	2.90	0.014

[a]Data from *Coadic et al.* [2013].

1999; *Johnstone et al.*, 2011; *Regenberg et al.*, 2014]. According to our observations, we adopt 21.3 ± 6.6 μmol/kg as the threshold $\Delta[CO_3^{2-}]$ for the dissolution effect on Mg/Ca [*Regenberg et al.*, 2014], and assume that B/Ca in *G. ruber* (w) and *G. sacculifer* (w/o sac) begins to be influenced by dissolution at the same $\Delta[CO_3^{2-}]$. It is notable that threshold $\Delta[CO_3^{2-}]$ for dissolution effect on B/Ca cannot be derived from our data set. However, as B/Ca values below the chosen threshold value are evidently lowered by dissolution, we can investigate the sensitivity of B/Ca change to bottom water $\Delta[CO_3^{2-}]$ using available data.

The sensitivity of B/Ca to $\Delta[CO_3^{2-}]$ varies between species in the different depth transects, from 0.69 to 0.90 μmol/mol per μmol/kg $\Delta[CO_3^{2-}]$ change for *G. sacculifer* (w/o sac) and 0.64 to 1.01 μmol/mol per μmol/kg $\Delta[CO_3^{2-}]$ change for *G. ruber* (w) for depth transects from this study (Figure 4). By comparison, B/Ca in *G. sacculifer* from Sierra Leone Rise is significantly less sensitive to bottom water $\Delta[CO_3^{2-}]$ change (0.32 μmol/mol per μmol/kg $\Delta[CO_3^{2-}]$ change) [*Coadic et al.*, 2013], which suggests that dissolution effect on B/Ca might vary at different locations.

To derive the sensitivity of B/Ca to bottom water $\Delta[CO_3^{2-}]$ change on a global scale, we translate initial B/Ca to ΔB/Ca, to represent the proportion of B/Ca strictly related to post depositional dissolution. We first define $B/Ca_{initial}$ as B/Ca of the sample at the threshold $\Delta[CO_3^{2-}]$, assuming that it is the B/Ca unaffected by dissolution. Using different threshold $\Delta[CO_3^{2-}]$ value to calculate ΔB/Ca at different depth transects would not affect our conclusion, as shown by sensitivity tests (supporting information Figure S1). $B/Ca_{initial}$ is calculated by extrapolating the regression line to the threshold $\Delta[CO_3^{2-}]$ at the Ontong Java Plateau and the southwestern Indian Ocean depth transects, and by averaging B/Ca above the threshold $\Delta[CO_3^{2-}]$ at the Caribbean Sea depth transect. Measured B/Ca is then translated to ΔB/Ca:

$$\Delta B/Ca = B/Ca_{measured} - B/Ca_{initial}.$$

Correlation between ΔB/Ca in both species from all three depth transects and $\Delta[CO_3^{2-}]$ is significant. The sensitivity of ΔB/Ca in *G. sacculifer* (w/o sac) to $\Delta[CO_3^{2-}]$ is 0.59 ± 0.13 μmol/mol per μmol/kg $\Delta[CO_3^{2-}]$ change ($r^2 = 0.51$, n = 22, $p < 0.001$, Figure 4c). ΔB/Ca from the Sierra Leone Rise (data from *Coadic et al.* [2013]) is systematically higher than ΔB/Ca from this study, and diverges from the trend defined by data from this study, possibly reflecting regional dependence of dissolution sensitivity. The sensitivity of ΔB/Ca in *G. ruber* (w) is 0.67 ± 0.22 μmol/mol per μmol/kg $\Delta[CO_3^{2-}]$ change ($r^2 = 0.45$, n = 15, $p = 0.009$, Figure 4d). These results, integrating data from different oceans, provide a first-order estimation of the sensitivity of B/Ca in *G. sacculifer* (w/o sac) and *G. ruber* (w) to dissolution effects.

4.4. Correlation With Coexisting Benthic B/Ca

The correlation of planktonic B/Ca in *G. sacculifer* (w/o sac) and *G. ruber* (w) with bottom water $\Delta[CO_3^{2-}]$ indicates that planktonic B/Ca can be corrected given the knowledge of bottom water $\Delta[CO_3^{2-}]$. As suggested by *Coadic et al.* [2013], for downcore reconstruction, an independent proxy for $\Delta[CO_3^{2-}]$ can be employed to correct for the dissolution effects on planktonic B/Ca. Given that benthic B/Ca is an established quantitative

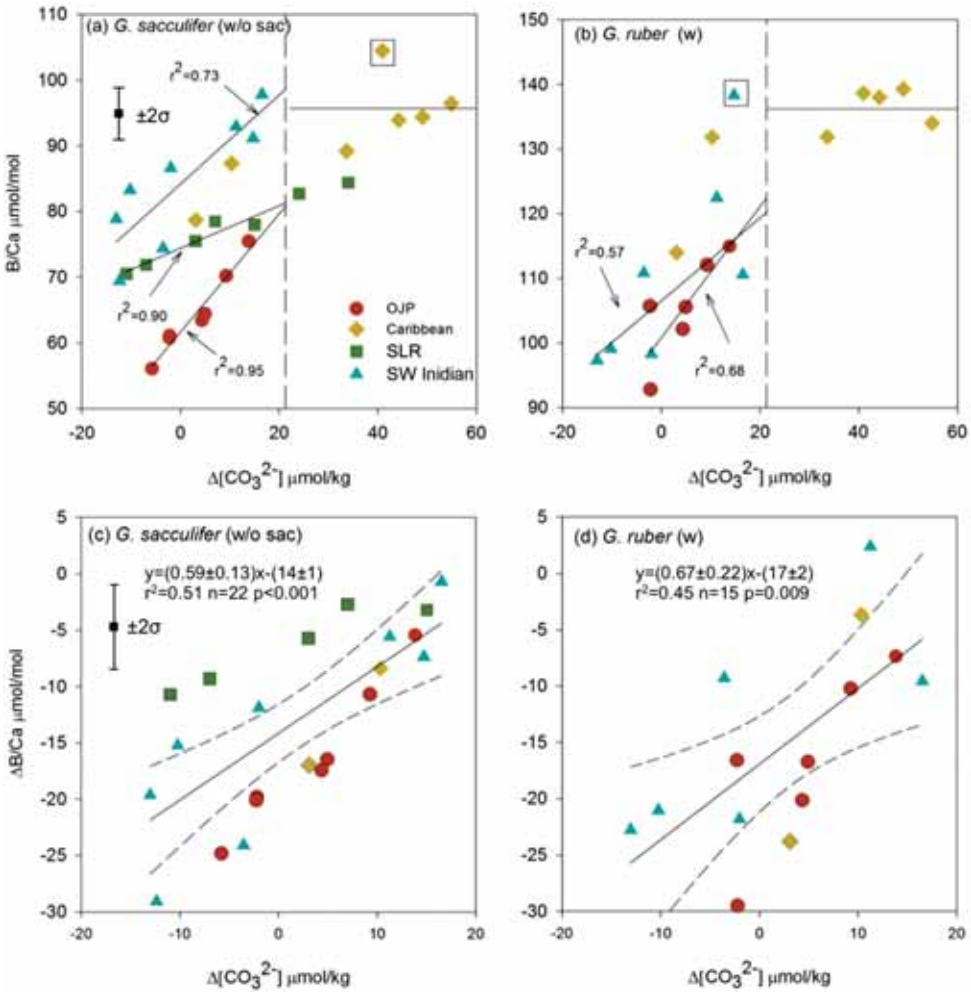

Figure 4. B/Ca in *G. sacculifer* (w/o sac) and *G. ruber* (w) versus bottom seawater $\Delta[CO_3^{2-}]$. Data from Sierra Leone Rise are from *Coadic et al.* [2013]. (a and b) Original B/Ca versus $\Delta[CO_3^{2-}]$, questionable data points are framed within boxes. Dashed lines indicate the threshold $\Delta[CO_3^{2-}]$ value for the onset discernable dissolution effects on Mg/Ca [*Regenberg et al.*, 2014]. For the Caribbean Sea data, black solid lines show the average B/Ca above the threshold $\Delta[CO_3^{2-}]$. Regression lines of data below threshold $\Delta[CO_3^{2-}]$ are extrapolated to threshold $\Delta[CO_3^{2-}]$ to estimate initial B/Ca. (c and d) ΔB/Ca versus $\Delta[CO_3^{2-}]$. Regression lines show average B/Ca loss rate with decreasing $\Delta[CO_3^{2-}]$. Dashed lines are the 95% confidence intervals. Error bar in Figures 4a and 4c represent $\pm 2\sigma$ range of the consistent standard.

proxy for bottom water $\Delta[CO_3^{2-}]$ change and is not affected by dissolution [*Yu and Elderfield*, 2007], it follows that $\Delta[CO_3^{2-}]$ reconstructed from the same sediment samples as planktonic B/Ca could be used to correct for the dissolution bias on planktonic B/Ca. Accordingly, here we attempt to use benthic B/Ca to evaluate how planktonic B/Ca records can be altered by bottom water $\Delta[CO_3^{2-}]$ change in sediment cores.

Sites with planktonic B/Ca evidently affected by dissolution are chosen for the following analysis. We begin by comparing our core-top planktonic B/Ca in *G. sacculifer* (w/o sac) and *G. ruber* (w) to published benthic B/Ca in *Cibicidoides wuellerstorfi* (data are from *Yu and Elderfield* [2007]) from the Ontong Java Plateau, the southwestern Indian Ocean, and the Caribbean Sea. We then translate planktonic and benthic B/Ca from different depth transects to relative changes within each depth transect. This makes data from different depth transects comparable:

$$B/Ca_{diff} = B/Ca_{measured} - B/Ca_{mean}.$$

It is revealed that all data from these three areas show a positive correlation between planktonic B/Ca and benthic B/Ca. B/Ca in *G. sacculifer* (w/o sac) and *G. ruber* (w) decreases 0.38 ± 0.11and 0.60 ± 0.07 μmol/mol per μmol/mol B/Ca change in *C. wuellerstorfi*, respectively (Figure 5).

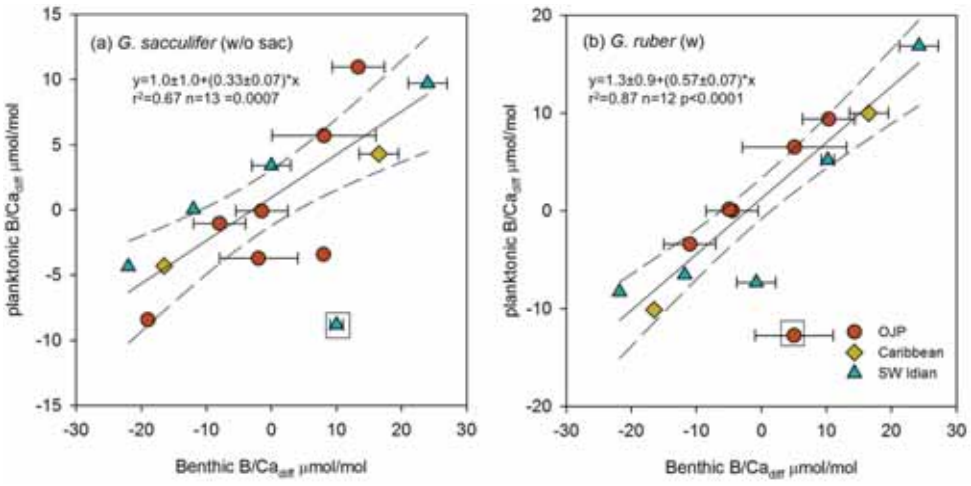

Figure 5. B/Ca in *G. sacculifer* (w/o sac) and *G. ruber* (w) versus coexisting B/Ca in *C. wuellerstorfi* [*Yu and Elderfield*, 2007]. Horizontal error bars indicate available standard errors of benthic B/Ca [*Yu and Elderfield*, 2007]. Questionable data points are framed within boxes and excluded from regression analysis. Solid lines and dashed lines are regression lines and 95% confidence internals, respectively, for the predicted planktonic B/Ca decline based on benthic B/Ca.

The comparison made above suggests that planktonic B/Ca change can be 35–55% of benthic B/Ca change. Glacial-interglacial difference of deep water $\Delta[CO_3^{2-}]$ can be as large as 50 μmol/kg, based on reconstructions from various proxies [*Broecker and Clark*, 2001b; *Marchitto et al*., 2005; *Yu et al*., 2010; *Doss and Marchitto*, 2013], which is equivalent to ~57 μmol/mol variation of B/Ca variations in *C. wuellerstorfi* [*Yu and Elderfield*, 2007]. According to the correlations shown in Figure 5, this would alter the planktonic B/Ca by 18–28 μmol/mol, if $\Delta[CO_3^{2-}]$ at a given site is always bathed in bottom water below the threshold $\Delta[CO_3^{2-}]$ value in order for planktonic B/Ca to decline. This dissolution effect is substantial compared to glacial-interglacial change in planktonic B/Ca of 25 μmol/mol [*Yu et al*., 2007a; *Foster*, 2008; *Palmer et al*., 2010; *Yu et al*., 2013]. With the sensitivity of planktonic B/Ca change to benthic B/Ca change here and the threshold $\Delta[CO_3^{2-}]$ value for planktonic B/Ca decline, it is feasible to correct for dissolution effects on planktonic B/Ca, if a benthic B/Ca record is available.

5. Conclusion

In this study, we have measured B/Ca in four planktonic foraminiferal species in core-top samples from three depth transects to investigate the effects of dissolution on planktonic foraminiferal B/Ca. We find that the dissolution effects on planktonic foraminiferal B/Ca are species-specific. Among the four species examined, B/Ca in *G. sacculifer* (w/o sac) and *G. ruber* (w) shows a significant decrease with progressive dissolution, while B/Ca in *N. dutertrei* and *P. obliquiloculata* is negligibly influenced by dissolution. The reason for species-specific responses of B/Ca in different species to dissolution might be related to the microscale distribution of B in foraminiferal shells. Decline of B/Ca in *G. sacculifer* (w/o sac) and *G. ruber* (w) is empirically correlated with bottom water $\Delta[CO_3^{2-}]$ and B/Ca of coexisting benthic foraminifera, which can provide an approach to correcting for dissolution effects on planktonic B/Ca downcore.

Acknowledgments
We thank Steve Eggins for suggestions and comments on an earlier draft. We thank Adina Paytan (the Editor), Eric Douville, and one anonymous reviewer for their thoughtful and detailed comments. The data used are listed in Table 1 and supporting information. This work is supported by ARC Discovery Project (DP140101393) and Future Fellowship (FT140100993) to J.Y.

References

Allen, K. A., B. Hönisch, S. M. Eggins, J. Yu, H. J. Spero, and H. Elderfield (2011), Controls on boron incorporation in cultured tests of the planktic foraminifer *Orbulina universa*, *Earth Planet. Sci. Lett.*, *309*(3–4), 291–301, doi:10.1016/j.epsl.2011.07.010.

Allen, K. A., B. Hönisch, S. M. Eggins, and Y. Rosenthal (2012), Environmental controls on B/Ca in calcite tests of the tropical planktic foraminifer species Globigerinoides ruber and *Globigerinoides sacculifer*, *Earth Planet. Sci. Lett.*, *351–352*, 270–280, doi:10.1016/j.epsl.2012.07.004.

Barker, S., M. Greaves, and H. Elderfield (2003), A study of cleaning procedures used for foraminiferal Mg/Ca paleothermometry, *Geochem. Geophys. Geosyst.*, *4*(9), 8407, doi:10.1029/2003GC000559.

Bassinot, F. C., F. Mélières, M. Gehlen, C. Levi, and L. Labeyrie (2004), Crystallinity of foraminifera shells: A proxy to reconstruct past bottom water $CO_3^{=}$ changes?, *Geochem. Geophys. Geosyst.*, *5*, Q08D10, doi:10.1029/2003GC000668.

Berger, W. H. (1970), Planktonic foraminifera: Selective solution and the lysocline, *Mar. Geol.*, *8*(2), 111–138.

Branson, O., S. A. T. Redfern, T. Tyliszczak, A. Sadekov, G. Langer, K. Kimoto, and H. Elderfield (2013), The coordination of Mg in foraminiferal calcite, *Earth Planet. Sci. Lett.*, *383*, 134–141, doi:10.1016/j.epsl.2013.09.037.

Branson, O., K. Kaczmarek, S. A. T. Redfern, S. Misra, G. Langer, T. Tyliszczak, J. Bijma, and H. Elderfield (2015), The coordination and distribution of B in foraminiferal calcite, *Earth Planet. Sci. Lett.*, *416*, 67–72, doi:10.1016/j.epsl.2015.02.006.

Broecker, W. S., and E. Clark (2001a), An evaluation of Lohmann's foraminifera weight dissolution index, *Paleoceanography*, *16*(5), 531–534, doi:10.1029/2000PA000600.

Broecker, W. S., and E. Clark (2001b), Glacial-to-Holocene redistribution of carbonate ion in the deep sea, *Science*, *294*(5549), 2152–2155.

Broecker, W. S., E. Clark, D. C. McCorkle, T.-H. Peng, I. Hajdas, and G. Bonani (1999), Evidence for a reduction in the carbonate ion content of the deep sea during the course of the Holocene, *Paleoceanography*, *14*(6), 744–752, doi:10.1029/1999PA900038.

Brown, S. J., and H. Elderfield (1996), Variations in Mg/Ca and Sr/Ca ratios of planktonic foraminifera caused by postdepositional dissolution: Evidence of shallow Mg-dependent dissolution, *Paleoceanography*, *11*(5), 543–551, doi:10.1029/96PA01491.

Coadic, R., F. Bassinot, D. Dissard, E. Douville, M. Greaves, and E. Michel (2013), A core-top study of dissolution effect on B/Ca in *Globigerinoides sacculifer* from the tropical Atlantic: Potential bias for paleo-reconstruction of seawater carbonate chemistry, *Geochem. Geophys. Geosyst.*, *14*, 1053–1068, doi:10.1029/2012GC004296.

Dekens, P. S., D. W. Lea, D. K. Pak, and H. J. Spero (2002), Core top calibration of Mg/Ca in tropical foraminifera: Refining paleotemperature estimation, *Geochem. Geophys. Geosyst.*, *3*(4), doi:10.1029/2001GC000200.

de Villiers, S. (2005), Foraminiferal shell-weight evidence for sedimentary calcite dissolution above the lysocline, *Deep Sea Res., Part I*, *52*(5), 671–680, doi:10.1016/j.dsr.2004.11.014.

Doss, W., and T. M. Marchitto (2013), Glacial deep ocean sequestration of CO_2 driven by the eastern equatorial Pacific biologic pump, *Earth Planet. Sci. Lett.*, *377–378*, 43–54, doi:10.1016/j.epsl.2013.07.019.

Edgar, K. M., E. Anagnostou, P. N. Pearson, and G. L. Foster (2015), Assessing the impact of diagenesis on δ11B, δ13C, δ18O, Sr/Ca and B/Ca values in fossil planktic foraminiferal calcite, *Geochim. Cosmochim. Acta*, *166*, 189–209, doi:10.1016/j.gca.2015.06.018.

Eggins, S., P. De Deckker, and J. Marshall (2003), Mg/Ca variation in planktonic foraminifera tests: Implications for reconstructing palaeo-seawater temperature and habitat migration, *Earth Planet. Sci. Lett.*, *212*(3–4), 291–306, doi:10.1016/S0012-821X(03)00283-8.

Elderfield, H., M. Vautravers, and M. Cooper (2002), The relationship between shell size and Mg/Ca, Sr/Ca, δ18O, and δ13C of species of planktonic foraminifera, *Geochem. Geophys. Geosyst.*, *3*(8), doi:10.1029/2001GC000194.

Foster, G. L. (2008), Seawater pH, pCO_2 and $[CO_3^{2-}]$ variations in the Caribbean Sea over the last 130 kyr: A boron isotope and B/Ca study of planktic foraminifera, *Earth Planet. Sci. Lett.*, *271*(1–4), 254–266, doi:10.1016/j.epsl.2008.04.015.

Gastrich, M. D. (1987), Ultrastructure of a new intracellular symbiotic alga found within planktonic foraminifera1, *J. Phycol.*, *23*(4), 623–632.

Hemleben, C., M. Spindler, and O. R. Anderson (1989), *Modern Planktonic Foraminifera*, Springer, N. Y.

Hemming, N. G., and G. N. Hanson (1992), Boron isotopic composition and concentration in modern marine carbonates, *Geochim. Cosmochim. Acta*, *56*(1), 537–543.

Hönisch, B., J. Bijma, A. D. Russell, H. J. Spero, M. R. Palmer, R. E. Zeebe, and A. Eisenhauer (2003), The influence of symbiont photosynthesis on the boron isotopic composition of foraminifera shells, *Mar. Micropaleontol.*, *49*(1–2), 87–96, doi:10.1016/S0377-8398(03)00030-6.

Johnstone, H. J. H., M. Schulz, S. Barker, and H. Elderfield (2010), Inside story: An X-ray computed tomography method for assessing dissolution in the tests of planktonic foraminifera, *Mar. Micropaleontol.*, *77*(1–2), 58–70, doi:10.1016/j.marmicro.2010.07.004.

Johnstone, H. J. H., J. Yu, H. Elderfield, and M. Schulz (2011), Improving temperature estimates derived from Mg/Ca of planktonic foraminifera using X-ray computed tomography–based dissolution index, XDX, *Paleoceanography*, *26*, PA1215, doi:10.1029/2009PA001902.

Key, R. M., A. Kozyr, C. L. Sabine, K. Lee, R. Wanninkhof, J. L. Bullister, R. A. Feely, F. J. Millero, C. Mordy, and T. H. Peng (2004), A global ocean carbon climatology: Results from Global Data Analysis Project (GLODAP), *Global Biogeochem.l Cycles*, *18*, GB4031, doi:10.1029/2004GB002247.

Lohmann, G. (1995), A model for variation in the chemistry of planktonic foraminifera due to secondary calcification and selective dissolution, *Paleoceanography*, *10*(3), 445–457.

Marchitto, T. M., J. Lynch-Stieglitz, and S. R. Hemming (2005), Deep Pacific $CaCO_3$ compensation and glacial–interglacial atmospheric CO_2, *Earth Planet. Sci. Lett.*, *231*(3–4), 317–336, doi:10.1016/j.epsl.2004.12.024.

Ni, Y., G. L. Foster, T. Bailey, T. Elliott, D. N. Schmidt, P. Pearson, B. Haley, and C. Coath (2007), A core top assessment of proxies for the ocean carbonate system in surface-dwelling foraminifers, *Paleoceanography*, *22*, PA3212, doi:10.1029/2006PA001337.

Nouet, J., and F. Bassinot (2007), Dissolution effects on the crystallography and Mg/Ca content of planktonic foraminifera *Globorotalia tumida* (Rotaliina) revealed by X-ray diffractometry, *Geochem. Geophys. Geosyst.*, *8*, Q10007, doi:10.1029/2007GC001647.

Palmer, M. R., G. J. Brummer, M. J. Cooper, H. Elderfield, M. J. Greaves, G. J. Reichart, S. Schouten, and J. M. Yu (2010), Multi-proxy reconstruction of surface water pCO_2 in the northern Arabian Sea since 29 ka, *Earth Planet. Sci. Lett.*, *295*(1–2), 49–57, doi:10.1016/j.epsl.2010.03.023.

Pelletier, G., E. Lewis, and D. Wallace (2005), *A Calculator for the CO2 System in Seawater for Microsoft Excel/VBA*, Wash. State Dep. of Ecol., Olympia.

Regenberg, M., D. Nürnberg, S. Steph, J. Groeneveld, D. Garbe-Schönberg, R. Tiedemann, and W.-C. Dullo (2006), Assessing the effect of dissolution on planktonic foraminiferal Mg/Ca ratios: Evidence from Caribbean core tops, *Geochem. Geophys. Geosyst.*, *7*, Q07P15, doi:10.1029/2005GC001019.

Regenberg, M., A. Regenberg, D. Garbe-Schönberg, and D. W. Lea (2014), Global dissolution effects on planktonic foraminiferal Mg/Ca ratios controlled by the calcite-saturation state of bottom waters, *Paleoceanography*, *19*, 127–142, doi:10.1002/2013PA002492.

Rollion-Bard, C., and J. Erez (2010), Intra-shell boron isotope ratios in the symbiont-bearing benthic foraminiferan Amphistegina lobifera: Implications for δ11B vital effects and paleo-pH reconstructions, *Geochim. Cosmochim. Acta*, *74*, 1530–1536, doi:10.1016/j.gca.2009.11.017.

Russell, A. D., S. Emerson, B. K. Nelson, J. Erez, and D. W. Lea (1994), Uranium in foraminiferal calcite as a recorder of seawater uranium concentrations, *Geochim. Cosmochim. Acta*, *58*(2), 671–681.

Sabine, C. L., R. A. Feely, N. Gruber, R. M. Key, K. Lee, J. L. Bullister, R. Wanninkhof, C. Wong, D. W. Wallace, and B. Tilbrook (2004), The oceanic sink for anthropogenic CO_2, *Science*, *305*(5682), 367–371.

Sadekov, A. Y., S. M. Eggins, and P. De Deckker (2005), Characterization of Mg/Ca distributions in planktonic foraminifera species by electron microprobe mapping, *Geochem. Geophys. Geosyst.*, *6*, Q12P06, doi:10.1029/2005GC000973.

Seki, O., G. L. Foster, D. N. Schmidt, A. Mackensen, K. Kawamura, and R. D. Pancost (2010), Alkenone and boron-based Pliocene pCO_2 records, *Earth Planet. Sci. Lett.*, *292*(1–2), 201–211, doi:10.1016/j.epsl.2010.01.037.

Wara, M. W., M. L. Delaney, T. D. Bullen, and A. C. Ravelo (2003), Possible roles of pH, temperature, and partial dissolution in determining boron concentration and isotopic composition in planktonic foraminifera, *Paleoceanography*, *18*(4), 1100, doi:10.1029/2002PA000797.

Wilson, D. J., A. M. Piotrowski, A. Galy, and I. N. McCave (2012), A boundary exchange influence on deglacial neodymium isotope records from the deep western Indian Ocean, *Earth Planet. Sci. Lett.*, *341–344*, 35–47, doi:10.1016/j.epsl.2012.06.009.

Yu, J., and H. Elderfield (2007), Benthic foraminiferal B/Ca ratios reflect deep water carbonate saturation state, *Earth Planet. Sci. Lett.*, *258*(1-2), 73–86, doi:10.1016/j.epsl.2007.03.025.

Yu, J., J. Day, M. Greaves, and H. Elderfield (2005), Determination of multiple element/calcium ratios in foraminiferal calcite by quadrupole ICP-MS, *Geochem. Geophys. Geosyst.*, *6*, Q08P01, doi:10.1029/2005GC000964.

Yu, J., H. Elderfield, and B. Hönisch (2007a), B/Ca in planktonic foraminifera as a proxy for surface seawater pH, *Paleoceanography*, *22*, PA2202, doi:10.1029/2006PA001347.

Yu, J., H. Elderfield, M. Greaves, and J. Day (2007b), Preferential dissolution of benthic foraminiferal calcite during laboratory reductive cleaning, *Geochem. Geophys. Geosyst.*, *8*, Q06016, doi:10.1029/2006GC001571.

Yu, J., W. S. Broecker, H. Elderfield, Z. Jin, J. F. McManus, and F. Zhang (2010), Loss of carbon from the deep sea since the LGM, *Science*, *330*, 1084–1087.

Yu, J., D. J. R. Thornalley, J. W. B. Rae, and N. I. McCave (2013), Calibration and application of B/Ca, Cd/Ca, and $\delta^{11}B$ in *Neogloboquadrina pachyderma* (sinistral) to constrain CO_2 uptake in the subpolar North Atlantic during the last deglaciation, *Paleoceanography*, *28*, 237–252, doi:10.1002/palo.20024.

Zeebe, R. E., D. A. Wolf-Gladrow, J. Bijma, and B. Hönisch (2003), Vital effects in foraminifera do not compromise the use of δ11B as a paleo-pH indicator: Evidence from modeling, *Paleoceanography*, *18*(2), 1043, doi:10.1029/2003PA000881.